Available online at www.sciencedirect.com
SCIENCE DIRECT®
ELSEVIER
International Journal of Mechanical Sciences 47 (2005) 1393–1408
International Journal of MECHANICAL SCIENCES
www.elsevier.com/locate/ijmecsci

Thermo-mechanical model of frictional self-excited vibrations

J. Awrejcewicz*, Yu. Pyryev

Department of Automatics and Biomechanics, Technical University of Lodz, Stefanowskiego 1/15, 90-924 Lodz, Poland

Received 10 December 2003; received in revised form 31 March 2005; accepted 12 May 2005
Available online 23 June 2005

Abstract

A novel thermo-mechanical model of frictional self-excited stick-slip vibrations is proposed. Contrary to the tribo-mechanical models known in literature, the proposed model does not include any massless elastic parts. The applied friction force depends on a relative velocity of the sliding bodies. The period of vibrations depends on both heating expansion conditions and on conditions of heat taking up (giving up). Stability of the stationary solutions is studied. A computation of contact parameters during heating of the bodies is performed. Possibility of the existence of frictional auto-vibrations is shown.

Keywords: Instability; Stick-slip; Frictional heating; Temperature

1. Introduction

There are numerous examples of autonomous systems exhibiting regular non-linear self-excited vibrations (see Fig. 1) carefully analysed in the literature.

The Froude pendulum serves as a classical dynamical system, frequently used in the mechanical literature, to illustrate generation of self-vibrations in a mechanical system with friction (Fig. 1a). Zhukowski [1] and Strelkov [2] analysed vibrations of a pendulum with friction attached to uniformly rotating bush, i.e. the so called Froude pendulum.

It has been proved by Wells and Thomas [3,4] that occurrence of stick-slip vibrations (after Bowden and Leben [5]) is associated with a difference between static and kinematic frictions. The

*Corresponding author. Tel.: +48 42 631 23 78; fax: +48 42 631 22 25.
E-mail address: awrejcew@p.lodz.pl (J. Awrejcewicz).

0020-7403/$ - see front matter
doi:10.1016/j.ijmecsci.2005.05.001

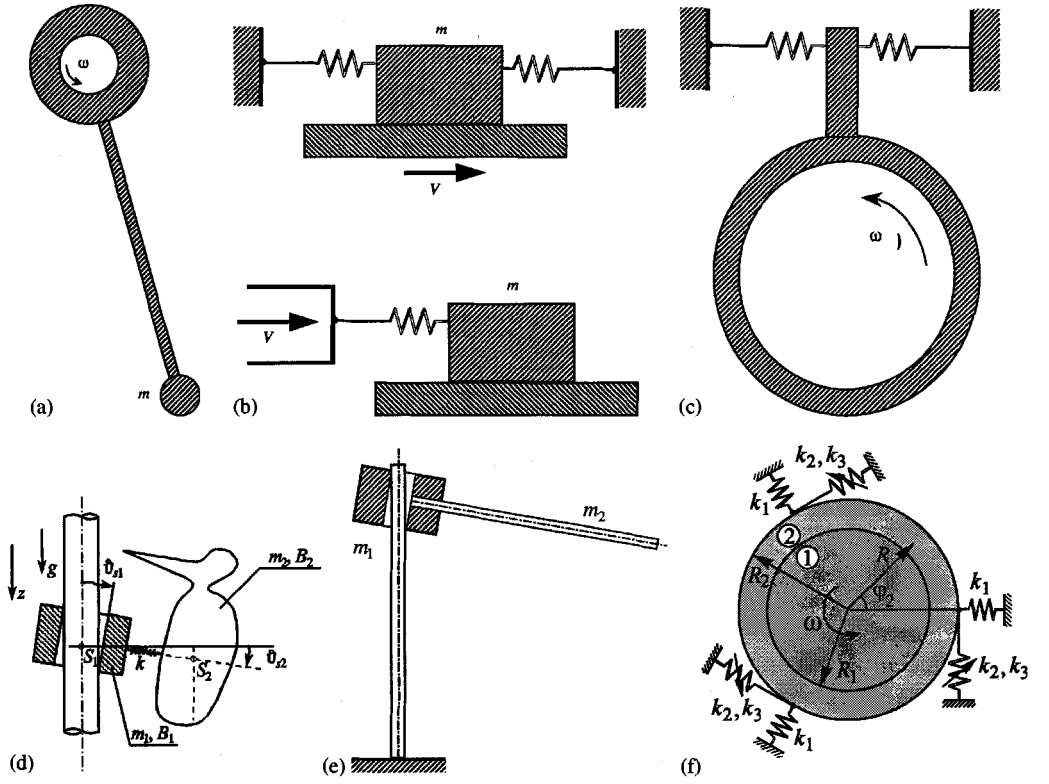

Fig. 1. Froude pendulum models (a); two (equivalent) sliding systems (b); Prony's clamp (c); woodpecker knocking into cylinder (d); the "Olędzki's slider" (e) and "cylinder-bush system" (f).

first model of self-excited vibrations was proposed by Van-der-Pol [6] (see Fig. 1b), and has been often applied since. The mathematical model shown in Fig. 1c is studied in references [7–9].

Stick-slip relaxation vibrations are studied in Ref. [10] with the use of the model shown in Fig. 1b as an example.

Note that for small motion velocities a static friction coefficient plays a key role, whereas for larger velocities, a kinematic friction coefficient is more important, which has been discussed and illustrated by Ishlinskiy [11]. The reader is encouraged to become familiar with the review references [12–15], where the history of the mentioned models and the ways of their investigation are included.

Vibrations of the mechanical system modelling the woodpecker behaviour (Fig. 1d) are analysed by Pfeiffer [16], and also studied in the monograph by Awrejcewicz [17]. The "mechanical woodpecker" consists of a stiff body with the moment of inertia B_2 and the mass m_2, and is coupled to a bush via a spring of stiffness k. The bush mass inertial moment is denoted by B_1.

Vibrations of the so-called "Olędzki's slider" were first studied in Ref. [18] (see Fig. 1e). If the mass centre S_2 of the horizontal rod is located at a distance larger than $l/(2f)$ (l denotes length of the slider, f is the friction coefficient), then (in static conditions) a motion of the rod or the slider

along the vertical rod—guide axis is not possible. However, an infinitely small perturbation of the end of the horizontal rod forces the system to move.

Note that two discussed models of the slider movement are associated with the "stick-slip" vibrational behaviour.

Despite considerable simplicity of the introduced models, important information is obtained. Namely, it is shown that a static self-braking kinematic pair can initiate movement, when the vibration appears.

Both regular and chaotic vibrations in a cylinder-bush system have been analysed by the authors [19,20].

It is worth noticing that the main conditions for occurrence of self-excited vibrations in the models discussed earlier are associated with a difference between static and kinematic frictions and with existence of an elastic coupling in a tribo-mechanical system.

It should be emphasized that both mathematical models and various methods applied to solve problems of contacting mechanical systems (one sided constraints) have been used separately so far. First, during analysis of dynamical models of the contacting mechanical systems tribologic processes (heat generation) occurring on the contacting surfaces of the considered bodies have been omitted. On the other hand, models of contacting bodies with an account of thermal effects usually do not include inertial forces of the bodies. The proposed paper fulfils the occurred gap in research devoted to this problem, since our proposed and illustrated models may be used to predict behaviour of real engineering contacting system.

It is clear that from an engineering point of view it is important to determine forces that occurred in kinematic pairs of the contacting bodies, as well as it is expected to obtain recipes for an optimal choice of frictional materials as well as other parameters required for realization of long time sure work of various elements of machines and mechanisms. Therefore, it is highly required that a progress in mathematical modelling of processes appeared in contacting systems yields finally the results being close to that observed in real systems.

In this work we analyse a mechanical problem governed by non-linear ordinary (ODE) and partial differential equations with the attached initial and boundary conditions. Owing to applied methodology, the stated problem is reduced to that of a system of ODEs and the integral equation modelling a contact pressure. The last equation is yielded by application of the Laplace transformation.

The frictional kinematic pair analysed by us can be applied into two qualitatively different mechanical objects: construction (coupling clips, conic frictional joints between a brake and hub and a pivot, coupling and brake design, flange and yielding packing) and experimental rigs (for instance, physical models of frictional machine heads).

Consider now our novel model, devoid of any elastic part but able to exhibit self-excited stick-slip vibrations (Fig. 2a). For simplicity, it will be further referred to as the "frog-slider".

The term "frog-slider" is introduced in order to emphasize that the body movement in the proposed model can be realized by jumps. In other words, the illustrated process includes two successive motion parts. Namely, after a relative "rest" of the system a "jump" occurs, when a frictional static force resistance is violated. Notice that friction force depends on both sliding velocity and heat transfer condition.

Many important questions concerning the system under investigation may be formulated. Which kinds of motion are possible? And how does heat and friction interact to create such

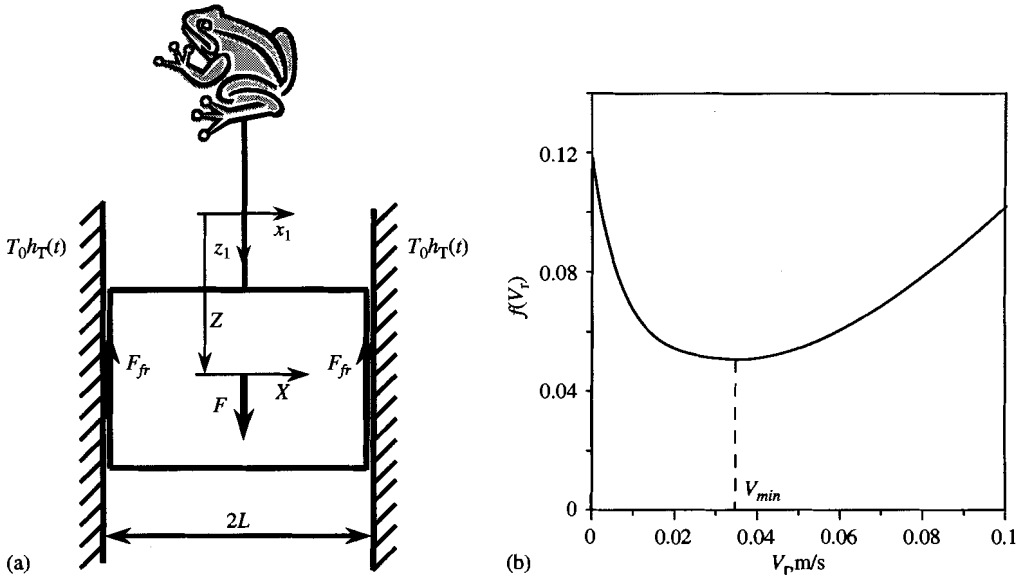

Fig. 2. "Frog-slider system" (a) and the Stribeck friction-speed curve (b).

motions? The answers to these questions are given in this paper. The considered body being in a contact or not (depending on the chosen parameters) may either be in: (i) an equilibrium state (friction force is larger than a driven force); (ii) a moment with constant velocity (friction force is equal to a driven force, and a generated heat is fully transformed into walls); (iii) stick-slip movement, and a stick regime (both body's temperature and contact pressure are decreased) is substituted by a slip regime (body heating and increase of contact pressure appear).

In this work a novel computational models is proposed, where variations of velocities is proposed, where variations of velocities of contacting bodies, contact pressure, friction force and temperature on a contacting surface are coupled and depend on each other. Numerical investigations indicate that the self-excited system being studied may exhibit either regular or 'stick-slip' vibrations. It is also expected that the detected phenomenon of the body braking owing to friction increase can be applied during design of the so-called "intelligent" brakes. Although the mentioned particular features of the frictional contacting pair dynamics have been presented separately by others in real mechanical systems, our proposed complex model is expected to be experimentally verified.

2. Statement of the problem

Let us consider a one-dimensional model of the thermo-elastic contact of a body with a surrounding medium. Assume that this body is represented by a rectangular plate ($l_1 \times l_2 \times 2L$) (Fig. 2a). The plate together with a "frog" of mass M_1 is subjected to force $F = F_* h_F(t)$ and moves vertically along walls in direction z_1 of the rectangular co-ordinates $0x_1y_1z_1$. At the initial instant, the body is situated at distance Z_0 and its velocity is $\dot{Z}_0$. The distance

between the walls is always equal to the initial plate thickness $2L$. The plate moves with non-constant velocity $\dot{Z}(t)$.

It is assumed that the heat conduction between the layer and the walls obeys Newton's law. At the initial instant the temperature is governed by the formula $T_0 h_T(t)$ ($h_T(t) \to 1$, $t \to \infty$). It causes heat extension of the parallelepiped in the direction of $0x_1$, and the body starts to contact the walls. In the result of this process, a frictional contact on the parallelepiped sides $X = \pm L$ occurs. A simple frictional model is applied in the further considerations, i.e. friction force F_{fr} is a product of normal reaction force $N(t)$ and a friction coefficient. That means that $F_{fr} = f(\dot{Z})N(t)$ is the friction force defining resistance of the movement of two sliding bodies. Here, contrary to the assumption made in Ref. [21], the kinematic friction coefficient $f(\dot{Z})$ depends on the relative velocity $V_r = \dot{Z}$ of the sliding bodies (Fig. 2b).

The friction force $\sigma_{XZ}(X, t)$ per unit contact surface $X = -L$, L generates heat. According to Ling's assumptions (cf. [22]), the work of the friction forces is transmitted into heat energy. Note that the non-contacting plate surfaces are heating isolated and have the dimensions of $L/l_1 \ll 1$, $L/l_2 \ll 1$, which stands in agreement with the assumption of our one-dimensional modelling.

In what follows the problem is reduced to determination of the mass plate centre displacement $Z(t)$, plate velocity $\dot{Z}(t)$, contact pressure $P(t) = N(t)/l_1 l_2 = -\sigma_{XX}(-L, t) = -\sigma_{XX}(L, t)$; plate temperature $T_1(X, t)$, and displacement $U(X, t)$ in the X-axis direction.

3. Mathematical problem formulation

In the considered case, the studied problem is governed by the dynamics of the plate mass centre [17]

$$m\ddot{Z}(t) = F_* h_F(t) - 2f(\dot{Z})P(t) \tag{1}$$

and equations of the heat stress theory for an isotropic body [23]

$$\frac{\partial}{\partial X}\left[\frac{\partial}{\partial X}U(X, t) - \alpha_1 \frac{1+\nu_1}{1-\nu_1} T_1(X, t)\right]^{\cdot} = 0, \tag{2}$$

$$\frac{\partial^2}{\partial X^2} T_1(X, t) = \frac{1}{a_1}\frac{\partial}{\partial t} T_1(X, t), \quad X \in (-L, L), \tag{3}$$

with the attached mechanical

$$U(-L, t) = 0, \quad U(L, t) = 0, \tag{4}$$

heat

$$-\lambda_1 \frac{\partial T_1(-L, t)}{\partial X} + \alpha_T(T_1(-L, t) - T_0 h_T(t)) = f(\dot{Z})\dot{Z}(t)P(t), \tag{5}$$

$$\lambda_1 \frac{\partial T_1(L, t)}{\partial X} + \alpha_T(T_1(L, t) - T_0 h_T(t)) = f(\dot{Z})\dot{Z}(t)P(t) \tag{6}$$

and initial

$$T(X,0)=0, \quad X\in(-L,L), \quad Z(0)=Z_0, \quad \dot{Z}(0)=\dot{Z}_0 \tag{7}$$

conditions. Normal stresses that occur in the plate are defined through

$$\sigma_{XX}=\frac{E_1}{1-2\nu_1}\left[\frac{1-\nu_1}{1+\nu_1}\frac{\partial U}{\partial X}-\alpha_1 T_1\right]. \tag{8}$$

In the above, the following notation is applied: E_1 is the elasticity modulus, ν_1, λ_1, a_1, α_1, α_T are Poisson's ratio, thermal conductivity, thermal diffusivity, thermal expansion and heat transfer coefficients, respectively; $m=M_1/l_1l_2$, whereas $P(t)=N(t)/l_1l_2$ denotes the contact pressure.

Integration of Eq. (2), with Eq. (8) and boundary conditions (4) taken into account, yields the contact pressure $P(t)=-\sigma_{XX}(-L,t)=-\sigma_{XX}(L,t)$:

$$P(t)=\frac{E_1\alpha_1T_0}{1-2\nu_1}\frac{1}{2L}\int_{-L}^{L}T_1(\xi,t)\,\mathrm{d}\xi. \tag{9}$$

Let us introduce the following similarity coefficients:

$$t_*=L^2/a_1[s], \quad \mathrm{v}_*=a_1/L[\mathrm{m\,s^{-1}}], \quad P_*=T_0E_1\alpha_1/(1-2\nu_1)[\mathrm{N\,m^{-2}}] \tag{10}$$

and the following non-dimensional parameters:

$$x=\frac{X}{L}, \quad \tau=\frac{t}{t_*}, \quad z=\frac{Z}{L}, \quad p=\frac{P}{P_*}, \quad \theta=\frac{T_1}{T_0}, \quad \varepsilon_1=\frac{2P_*t_*^2}{mL}, \tag{11}$$

$$\gamma=\frac{E_1\alpha_1a_1}{(1-2\nu_1)\lambda_1}, \quad Bi=\frac{L\alpha_T}{\lambda_1}, \quad m_0=\frac{F_*}{2P_*}, \quad F(\dot{z})=f(\mathrm{v}_*\dot{z}). \tag{12}$$

The examined problem is modelled by means of non-dimensional equations of the form

$$\frac{\partial^2\theta(x,\tau)}{\partial x^2}=\frac{\partial\theta(x,\tau)}{\partial\tau}, \quad x\in(-1,\,1), \quad \tau\in(0,\,\infty), \tag{13}$$

$$\ddot{z}(\tau)=\varepsilon_1(m_0h_F(\tau)-F(\dot{z})p(\tau)), \tag{14}$$

with the following boundary

$$\left[\frac{\partial\theta(x,\tau)}{\partial x}-Bi\theta(x,\tau)\right]_{x=-1}=-q(\tau),$$
$$\left[\frac{\partial\theta(x,\tau)}{\partial x}+Bi\theta(x,\tau)\right]_{x=1}=q(\tau) \tag{15}$$

and initial

$$\theta(x,0)=0, \quad z(0)=z^\circ, \quad \dot{z}(0)=\dot{z}^\circ, \tag{16}$$

conditions, where

$$q(\tau)=Bih_T(\tau)+\gamma F(\dot{z})\dot{z}(\tau)p(\tau), \quad p(\tau)=\frac{1}{2}\int_{-1}^{1}\theta(\xi,\tau)\,\mathrm{d}\xi. \tag{17}$$

4. Solution of the problem

Applying the Laplace transformation [24]

$$\{\bar{\theta},\bar{p},\bar{q}\} = \int_0^\infty \{\theta,p,q\}\mathrm{e}^{-s\tau}\,\mathrm{d}\tau$$

the following is obtained:

$$\frac{\mathrm{d}^2\bar{\theta}}{\mathrm{d}x^2} = s\bar{\theta}, \tag{18}$$

$$\left[\frac{\mathrm{d}\bar{\theta}}{\mathrm{d}x} - Bi\bar{\theta}\right]_{x=-1} = -\bar{q}, \quad \left[\frac{\mathrm{d}\bar{\theta}}{\mathrm{d}x} + Bi\bar{\theta}\right]_{x=1} = \bar{q}, \tag{19}$$

$$\bar{p} = \frac{1}{2}\int_{-1}^{1} \bar{\theta}(\xi,s)\,\mathrm{d}\xi. \tag{20}$$

A solution to Eq. (18) is sought in the form

$$\bar{\theta}(x,s) = A(s)\bar{S}(x,s) + B(s)\bar{C}(x,s), \tag{21}$$

where

$$\bar{S}(x,s) = \sinh(\sqrt{s}x)/\sqrt{s}, \quad \bar{C}(x,s) = \cosh(\sqrt{s}x).$$

Quantities $A(s)$ and $B(s)$ are defined through two boundary value problems (19). Finally, we get

$$\bar{\theta}(x,s) = s\bar{q}(s)\bar{G}_\theta(x,s), \quad \bar{p}(s) = s\bar{q}(s)\bar{G}_p(s), \tag{22}$$

where

$$\bar{G}_p(x,s) = \frac{\bar{S}(s)}{s\Delta_1(s)}, \quad \bar{G}_\theta(x,s) = \frac{\bar{C}(x,s)}{s\Delta_1(s)},$$

$$\Delta_1(s) = s\bar{S}(s) + Bi\bar{C}(s),$$

$$\bar{S}(s) = \sinh(\sqrt{s})/\sqrt{s}, \quad \bar{C}(s) = \cosh(\sqrt{s}). \tag{23}$$

Applying an inverse Laplace transformation, the following system of equations is obtained:

$$p(\tau) = Bi\int_0^\tau \dot{h}_T(\xi)G_p(\tau-\xi)\,\mathrm{d}\xi + \gamma\int_0^\tau F(\dot{z})\dot{z}(\xi)p(\xi)\dot{G}_p(\tau-\xi)\,\mathrm{d}\xi, \tag{24}$$

$$\dot{z}(\tau) = \varepsilon_1\left[m_0\int_0^\tau h_F(\xi)\,\mathrm{d}\xi - \int_0^\tau F(\dot{z})p(\xi)\,\mathrm{d}\xi\right], \tag{25}$$

which yields non-dimensional pressure $p(\tau)$ and velocity $\dot{z}(\tau)$. The temperature is defined through the following formula:

$$\theta(x,\tau) = Bi\int_0^\tau \dot{h}_T(\xi)G_\theta(x,\tau-\xi)\,\mathrm{d}\xi + \gamma\int_0^\tau F(\dot{z})\dot{z}(\xi)p(\xi)\dot{G}_\theta(x,\tau-\xi)\,\mathrm{d}\xi, \tag{26}$$

where

$$\{G_p(\tau),\ G_\theta(1,\tau)\} = \frac{1}{Bi} - \sum_{m=1}^{\infty} \frac{\{2Bi,\ 2\mu_m^2\}}{\mu_m^2[Bi(Bi+1)+\mu_m^2]} e^{-\mu_m^2\tau} \tag{27}$$

and μ_m are the roots of the following characteristic equation:

$$tg\mu_m = \frac{Bi}{\mu_m}, \quad m = 1,2,\ldots\ . \tag{28}$$

Observe that $\mu_m \approx \pi m$, $m \to \infty$.

Notice that it is easy to formulate dependence between the heat flow and the contact pressure velocity variation in the form

$$\frac{dp(\tau)}{d\tau} = \left.\frac{\partial\theta(\tau,x)}{\partial x}\right|_{x=1}, \tag{29}$$

which will be used further in the analysis of the contact characteristics.

In order to carry out a numerical analysis, the knowledge of function (27) is required. The values of function (27) for $\tau \to 0$ and ∞ are defined via application of the theorem on the limiting values (cf. [25]):

$$\{G_p(\tau), G_\theta(1,\tau)\} \approx 1/Bi, \quad \tau \to \infty, \tag{30}$$

$$G_p(\tau) \approx \tau, \quad G_\theta(1,\tau) = 2\sqrt{\tau}/\sqrt{\pi}, \quad \tau \to 0. \tag{31}$$

5. Steady-state solution analysis

A stationary solution to the problem reads:

$$p_{st} = \frac{1}{1-\mathrm{v}}, \quad \theta_{st} = \frac{1}{1-\mathrm{v}}, \quad \mathrm{v} \doteq F(\mathrm{v}_{st})\frac{v_{st}\gamma}{Bi}, \tag{32}$$

where v_{st} is the solution of the non-linear equation

$$F(\mathrm{v}_{st}) = \frac{m_0}{1+\gamma m_0 \mathrm{v}_{st}/Bi}. \tag{33}$$

Graphical solution of Eq. (33) is presented in Fig. 3 for various parameters m_0 and Bi. Recall that for steel $\gamma = 1.87$.

The right-hand side of Eq. (33) is represented by solid curves for different values of parameter m_0 and Bi. Solid curve 1 is associated with parameter $m_0 = 0.14$, $Bi = 20$, solid curve 2—$m_0 = 0.1$, $Bi = 20$, solid curve 3—$m_0 = 0.1$, $Bi = 5$, solid curve 4—$m_0 = 0.14$, $Bi = 5$. The dashed curve is associated with function $F(\mathrm{v}_{st})$.

For different values of the parameters Eq. (33) can have a different number of solutions: for $m_0 = 0.14$, $Bi = 20$ (first case) it has one solution v_{st}^3 ($F'(\mathrm{v}_{st}^3) > 0$), for $m_0 = 0.1$, $Bi = 20$ (second

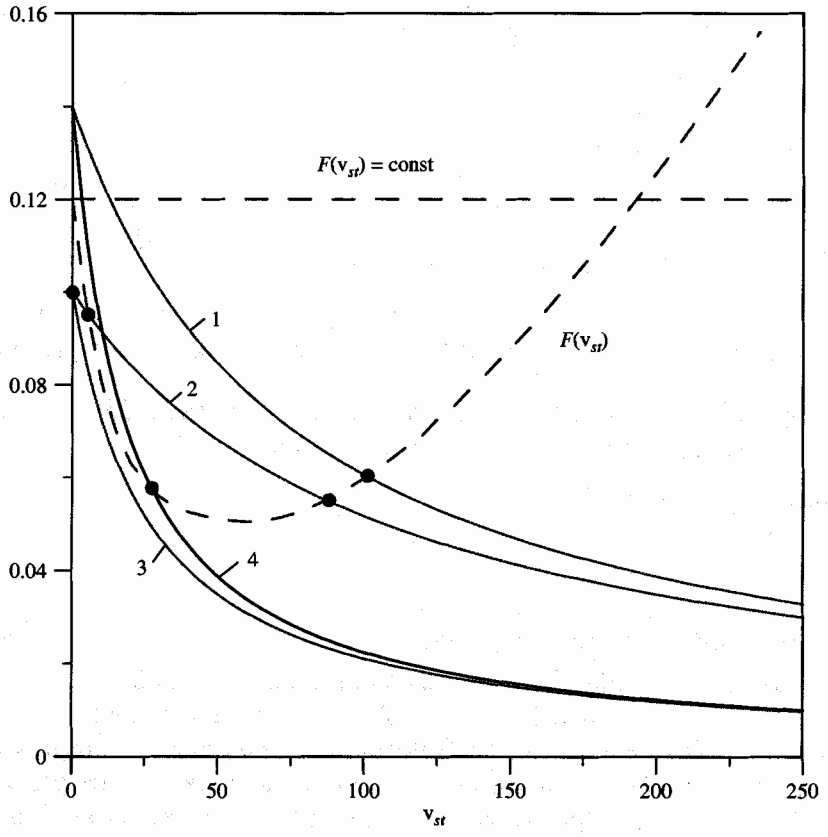

Fig. 3. Graphical solution of Eq. (33).

case)—three solutions v_{st}^1, v_{st}^2, v_{st}^3 ($F'(v_{st}^1)>0$, $F'(v_{st}^2)<0$, $F'(v_{st}^3)>0$), and for $m_0 = 0.1$, $Bi = 5$ (third case) one solution $v_{st}^1 = 0$ (with approximation (44) $v_{st}^1 \approx \varepsilon_0 m_0/2F_0$, $F'(v_{st}^1) \approx 2F_0/\varepsilon_0$). For $m_0 = 0.14$, $Bi = 5$ (fourth case)—again one solution exists v_{st}^2 ($F'(v_{st}^2)<0$).

The case of constant friction presented in Fig. 3 by the dashed horizontal line $F(v_{st}) = f = const$ was earlier considered in Ref. [21], where $v_{st} = Bi(m_0/f - 1)/(m_0\gamma)$.

Let us introduce a perturbation of the stationary solution (32) by means of the following formulas:

$$\dot{z} = v_{st} + \dot{z}^*, \quad p = p_{st} + p^*, \quad \theta = \theta_{st} + \theta^*, \quad h_T = 1 + h_T^*. \tag{34}$$

Owing to the linearization of the right-hand sides of Eq. (14) and with boundary condition (15) taken into account, the following linear problem is obtained:

$$\frac{\partial^2\theta^*(x,\tau)}{\partial\tau^2} = \frac{\partial\theta^*(x,\tau)}{\partial\tau}, \tag{35}$$

$$\ddot{z}^*(\tau) = \varepsilon_1[-F(v_{st})p^*(\tau) - F'(v_{st})p_{st}\dot{z}^*], \tag{36}$$

$$\left[\frac{d\theta^*(x,\tau)}{dx} - Bi\theta^*(x,\tau)\right]_{x=-1} = -q^*(\tau), \tag{37}$$

$$\left[\frac{d\theta^*(x,\tau)}{dx} + Bi\theta^*(x,\tau)\right]_{x=1} = q^*(\tau), \tag{38}$$

where

$$q^*(\tau) = Bih_T^*(\tau) + \gamma(v_{st}p_{st}(\beta_1+\beta_2)\dot{z}^*(\tau) + v_{st}F(v_{st})p^*(\tau)),$$

$$p^*(\tau) = \frac{1}{2}\int_{-1}^{1}\theta^*(\xi,\tau)\,d\xi, \quad \beta_1 = \frac{F(v_{st})}{v_{st}}, \quad \beta_2 = F'(v_{st}). \tag{39}$$

Further, applying the Laplace transformation, a solution of problem (35)–(39) in the transform domain is found. For example, the pressure perturbation reads:

$$p^*(s) = \frac{\bar{S}(s)Bi(\beta_2 p_{st}\varepsilon_1 + s)}{\Delta(s)}h_T^*(s), \tag{40}$$

where

$$\Delta(s) = (\varepsilon_1 p_{st}\beta_2 + s)\Delta_1(s) + Biv(\varepsilon_1 p_{st}\beta_1 - s)\bar{S}(s) = 0 \tag{41}$$

is the characteristic equation of the linearized problem. The roots s_m ($Re\,s_1 > Re\,s_2 > \cdots > Re\,s_m > \cdots$, $m = 1,2,3,\ldots$) of characteristic (41) lie either in the left-hand side of the complex plane $Re\,s<0$ (stationary solution is stable) or in the right-hand side of the complex plane $Re\,s>0$ (stationary solution is unstable) of the complex variable s.

The characteristic function $\Delta(s)$, in the form of an infinite order polynomial, is

$$\Delta(s) = \sum_{m=0}^{\infty} s^m b_m, \tag{42}$$

where

$$b_0 = \varepsilon_1 p_{st}c_0, \quad b_m = \varepsilon_1 p_{st}c_m + d_{m-1}, \quad m = 1,2,\ldots$$

$$c_0 = Bi(\beta_2 + v\beta_1), \quad d_m = d_m^{(1)} - Biv d_m^{(2)}, \quad c_m = \beta_2 d_m^{(1)} + Biv\beta_1 d_m^{(2)},$$

$$d_m^{(1)} = \frac{2m+Bi}{(2m)!}, \quad d_m^{(2)} = \frac{1}{(2m+1)!}.$$

Observe that in the analysis of the roots of characteristic (41), parameter v_{st} represents a solution of non-linear (33). Furthermore, note that in accordance with Eq. (32), $0<v<1$. It is easy to prove that $d_m>0$ ($m = 0,1,2,\ldots$) and $b_m>0$ if $\beta_2 \geqslant 0$.

Assuming that the body moves with a constant velocity, $v_{st} = const$, the so-called frictional thermo-elastic instability occurs ($Re\,s_1>0$) for $v>1$. The latter is characterised by an exponential increase of the contact characteristics, and the moving body is overheated.

In this case, the examination concerns the steel made parallelepiped plate ($\alpha_1 = 14\times10^{-6}\,°C^{-1}$, $\lambda_1 = 21W/(m\,°C^{-1})$, $\nu_1 = 0.3$, $a_1 = 5.9\times10^{-6}\,m^2\,s^{-1}$, $E_1 = 19\times10^{10}\,Pa$) with $L = 0.01\,m$, $T_0 = 5\,°C$, $z^\circ = \dot{z}^\circ = 0$ and with a non-constant friction coefficient. The result is $t_* = 16.95\,s$,

$v_* = 0.59 \times 10^{-3}\,\mathrm{m\,s^{-1}}$, $P_* = 3.3 \times 10^7\,\mathrm{Pa}$. The function $F(\dot{z}) = f(v_*\dot{z})$ is defined through the formula (cf. [20])

$$f(v_r) = \mathrm{sgn}(v_r)\begin{cases} f_{min} + (F_0 - f_{min})\exp(-b_1|v_r|) & \text{for } |v_r| < v_{min}, \\ [-F_0; F_0] & \text{for } v_r = 0, \\ f_{min} + (F_0 - f_{min})\exp(-b_1|v_{min}|) & \\ \quad + \frac{b_2 b_3 (|v_r| - v_{min})^2}{1 + b_2(|v_r| - v_{min})} & \text{for } |v_r| > v_{min}, \end{cases} \tag{43}$$

where $F_0 = 0.12, f_{min} = 0.05, b_1 = 140\,\mathrm{s\,m^{-1}}, b_2 = 10\,\mathrm{s\,m^{-1}}, b_3 = 2\,\mathrm{s\,m^{-1}}, v_{min} = 0.035\,\mathrm{m\,c^{-1}}$. The function $\mathrm{sgn}(x)$ is approximated through formula (cf. [14])

$$\mathrm{sgn}_{\varepsilon_0}(x) = \begin{cases} 1 & \text{if } x > \varepsilon_0, \\ \left(2 - \dfrac{|x|}{\varepsilon_0}\right)\dfrac{x}{\varepsilon_0} & \text{if } |x| < \varepsilon_0, \\ -1 & \text{if } x < -\varepsilon_0, \end{cases} \tag{44}$$

where $\varepsilon_0 = 0.0001$.

In the first case (for $m_0 = 0.14$, $Bi = 20$), one solution $v^3_{st} = 101.1$, $p^3_{st} = 2.32$, $\theta^3_{st} = 2.32$, ($\beta_1 = 0.6 \times 10^{-3}$, $\beta_2 = 0.4 \times 10^{-3}$, $v = 0.57$) is found. It is always stable (for instance, for $\varepsilon_1 = 800$ the roots of Eq. (41) $s_{1,2} = -1.02 \pm 1.57i$, whereas for $\varepsilon_1 = 75.45$ the roots of Eq. (41) $s_1 = -0.57$ lie in the left-hand side of the complex variable s). In this case after a transitional process, the body starts to move with constant velocity $v^3_{st} = 101.1$. The contact characteristics for $\varepsilon_1 = 800$ achieve their limiting values through the damped oscillation process with the expected 'period' $T = 4$, whereas for $\varepsilon_1 < 75.45$ the contact characteristics are overdamped.

In the second case ($m_0 = 0.1$, $Bi = 20$), three solutions appear. The solution $v^3_{st} = 87.1$, $p^3_{st} = \theta^3_{st} = 1.8$, $\theta^3_{st} = 2.25$, ($\beta_1 = 0.6 \times 10^{-3}$, $\beta_2 = 0.3 \times 10^{-3}$, $v = 0.45$) is stable (for instance, for $\varepsilon_1 = 800$ the roots of Eq. (41) $s_{1,2} = -0.93 \pm 1.1i$ lie in the left-hand side of the complex plane s). The solution $v^2_{st} = 5.26$ ($\beta_1 = 0.2 \times 10^{-1}$, $\beta_2 = -0.4 \times 10^{-2}$, $v = 0.05$) can be unstable (for instance for $\varepsilon_1 = 800$ the root of Eq. (41) $s_1 = 2.84$). The solution described through approximation (44) $v^1_{st} = 0.4 \times 10^{-4}$ ($\beta_1 = \beta_2 = 2.4 \times 10^3$, $v = 4 \times 10^{-7}$) corresponds to the equilibrium state (roots of Eq. (41) $s_1 = -2.2$, $s_2 = -20$ lie in the left-hand side of the complex plane). In the considered case, the contact characteristics for $\varepsilon_1 = 800$ tend, depending on initial conditions, to one of the two stable solutions.

In the third case ($m_0 = 0.1$, $Bi = 5$), there is only one solution. The approximation of the solution given by Eq. (44) $v^1_{st} = 0.4 \times 10^{-4} \approx 0$, $p^1_{st} = 1.0$, $\theta^1_{st} = 1.0$, ($\beta_1 = \beta_2 = 2.4 \times 10^3$, $v = 1.5 \times 10^{-6}$) corresponds to the equilibrium state (for $\varepsilon_1 = 800$ roots of Eq. (41) $s_1 = -1.7$, $s_2 = -16.3$ lie in the left-hand side of the complex plane). Notice that in this case, there always occurs a braking process (the applied external force is smaller than the friction force).

In the fourth case ($m_0 = 0.14$, $Bi = 5$), the only solution that exists is of the form: $v^2_{st} = 27.8$, $p^2_{st} = \theta^2_{st} = 2.45$, ($\beta_1 = 0.2 \times 10^{-2}$, $\beta_2 = -0.58 \times 10^{-3}$, $v = 0.59$). It is unstable if parameter ε_1 is larger than its critical value ($\varepsilon_1 \geqslant \tilde{\varepsilon}$). One may use characteristic function (42) for $m = 3$ to estimate a stability zone of the stationary solution of Eq. (32). Recall that one of the conditions for the cubic characteristic equation roots to lie on the right-hand side of the complex plane is exhibited by the inequality $b_1 b_2 - b_0 b_3 < 0$. In the discussed case it results in the following

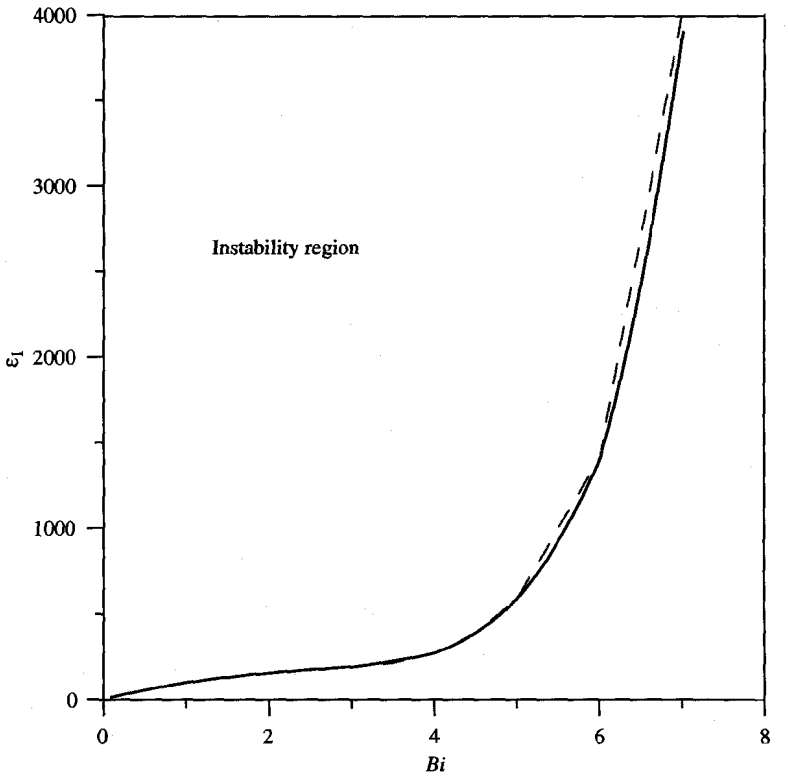

Fig. 4. Critical parameter ε_1 vs. *Bi*.

instability occurrence condition:

$$\varepsilon_1 > \tilde{\varepsilon}, \quad \tilde{\varepsilon} = (1 - \nu)(-B - \sqrt{B^2 - 4AC})/(2A), \tag{45}$$

where $A = c_1c_2 - c_0c_3$, $B = c_1d_1 + c_2d_0 - c_0d_2$, $C = d_0d_1$. In Fig. 4 the dashed curve represents dependence of function $\tilde{\varepsilon}$ on parameter *Bi*. The stability loss curve derived through the characteristic Eq. (41) analysis is denoted by the solid line. Observe that for the considered parameters, a good agreement in the unstable zone estimation through Eqs. (41) and (42) for $m = 3$ is achieved. Furthermore, the associated analytical formula is given. An increase of the heat taking up (increase of non-dimensional parameter *Bi*) causes an increase of critical parameter $\tilde{\varepsilon}$ (stable solution zone is increased). Moreover, for any fixed material body and for its loading parameters there is parameter *Bi* such that a stationary solution is always stable (in the considered case $Bi > 8$).

The period of oscillation vs. *Bi* is shown in Fig. 5a. An increase of *Bi* causes variation in the period oscillation (first it is decreased, then increased, and then again decreased).

In Fig. 5b, the dependence of the solution to Eq. (33) on parameter *Bi* is shown. Note that a physical sense of non-dimensional stationary velocity v_{st} exists for $\varepsilon_1 < \tilde{\varepsilon}$.

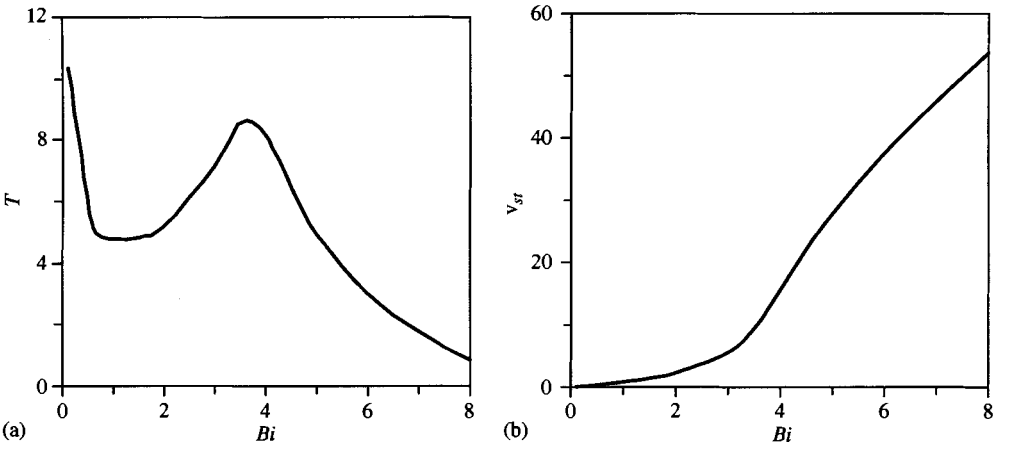

Fig. 5. Dimensionless period T vs. Bi (a) and dimensional velocity v_{st} vs. Bi.

6. Numerical analysis of the transient solution

Let us take the fourth case as an example. Here, for $\varepsilon_1 = 400$ ($\varepsilon_1 < \tilde{\varepsilon}$) the roots of Eq. (41) $s_{1,2} = -0.12 \pm 1.06i$ lie in the left-hand side of the complex plane s, and a solution is exhibited through 'periodic' damped oscillation (expected period $T = 2\pi/Im\, s_1 = 5.94$). For the critical value $\varepsilon_1 \approx \tilde{\varepsilon} = 587$, the roots $s_{1,2} = \pm 1.29i$ lie on the imaginary axis, and the expected period is $T = 4.87$. For $\varepsilon_1 = 800$, the roots $s_{1,2} = 0.14 \pm 1.5i$ lie in the right-hand side of the complex plane s. A stationary solution is unstable, and a limiting stick-slip cycle appears with the expected period $T = 4.18$.

In order to confirm the given conclusions, a numerical analysis is carried out for the fourth case for $Bi = 5$ (now $\varepsilon_1 \approx \tilde{\varepsilon} = 586.5$), and the computational results are shown in Figs. 6 and 7 for a few values of parameter $\varepsilon_1 = 400$; 586.5; 800. Fig. 6a shows the dependence of non-dimensional body velocity $\dot{z}(\tau)$ on non-dimensional time τ is shown. Curve 1 corresponds to the case when $\varepsilon_1 = 800$ ($m = 2.4 \times 10^9 \,\mathrm{kg\,m^{-2}}$), curve 2 illustrates the case $\varepsilon_1 = 586.5$ ($m = 3.25 \times 10^9 \,\mathrm{kg\,m^{-2}}$), and curve 3 is for $\varepsilon_1 = 400$ ($m = 4.8 \times 10^{10} \,\mathrm{kg\,m^{-2}}$). In Fig. 6b, the time history of non-dimensional friction force $\varepsilon_1 F(\dot{z}) p(\tau)$ occurring in the right-hand side of Eq. (14) is shown.

The time evolution of both non-dimensional contact pressure $p(\tau)$ and temperature $\theta(-1, \tau) = \theta(1, \tau)$ is reported in Figs. 7a and b (curve 1: $\varepsilon_1 = 800$; curve 2: $\varepsilon_1 = 586.5$; curve 3: $\varepsilon_1 = 400$).

As Figs. 6 and 7 show, the contact characteristics either have damped oscillatory shape (curves 3) approaching stationary states or they are periodic (curves 2) or stick-slip periodic (curves 1). The performed numerical analysis confirms the theoretical prediction. It is found that: $v_{st}^2 = 27.8$, $p_{st}^2 = \theta_{st}^2 = 2.45$. In the case associated with curves 1, the period of stick-slip contact periodic oscillations $T = 2.7$. In the critical case $T = 4.1$, for $\varepsilon_1 = 400$ (curve 3) the period of damped oscillations $T = 2.7$.

In order to facilitate the analysis of the stick-slip contact characteristics ($\varepsilon_1 = 800$), the associated periodic orbits are shown in Fig. 8.

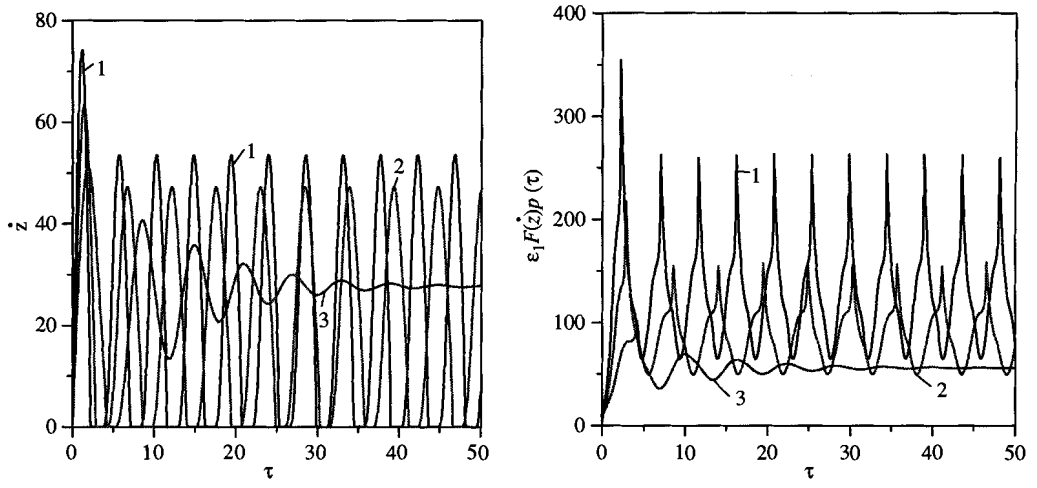

Fig. 6. Time history of non-dimensional body's velocity (a) and friction force (b) for various values of ε_1.

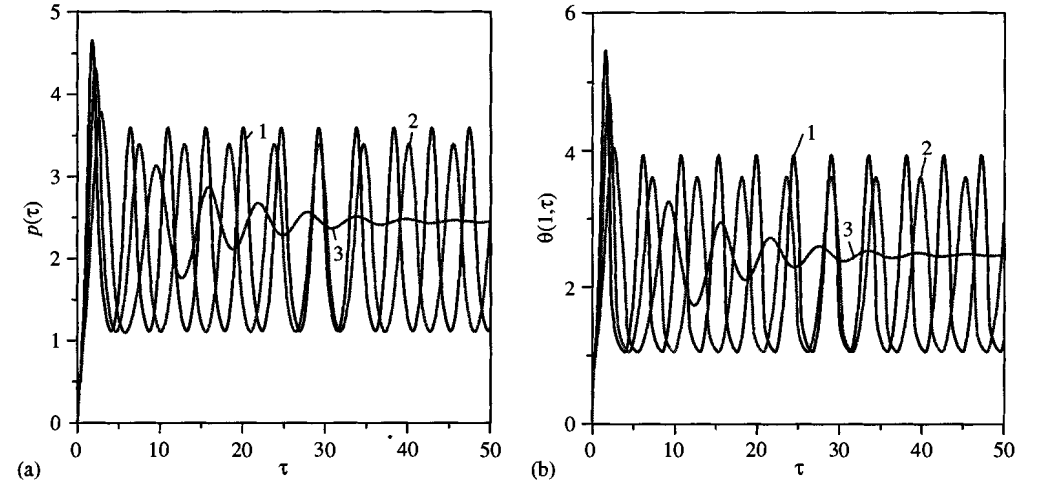

Fig. 7. Time history of non-dimensional contact pressure (a) and temperature (b) for various values of ε_1.

Note that the period of oscillations T includes slip phase t_{sl} and stick phase t_{st} ($T = t_{sl} + t_{st}$). The slip phase, consisting of acceleration ($\ddot{z} > 0$) and braking, begins at the time instant when the friction force $\varepsilon_1 F(\dot{z})p(\tau)$ is smaller than the force $\varepsilon_1 m_0$ applied to the body. Beginning from this time instant, both the body velocity and the contact temperature increase, but $\dot{p}(\tau) < 0$ (owing to formula (29) the body is cooled). At the time instant corresponding to $\dot{p}(\tau) = 0$, the heat stream equals zero and the body starts to be heated. Since heat expansion increases, the contact pressure increases as well. The kinetic friction coefficient $F(\dot{z})$ goes down, the friction force $\varepsilon_1 F(\dot{z})p(\tau)$ also decreases initially since the contact pressure increases slightly. Further pressure increase causes friction increase. When the friction force achieves the value of the external force $\varepsilon_1 m_0$, the body velocity achieves its maximum and the braking begins ($\ddot{z} < 0$) while the kinematic friction

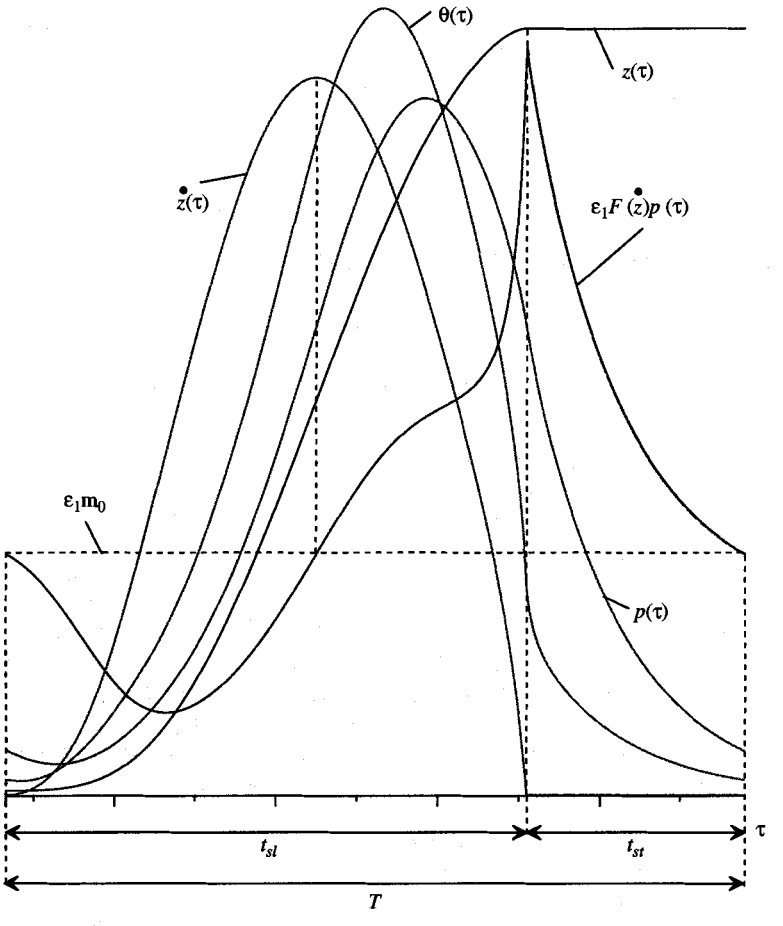

Fig. 8. T-periodic oscillations of non-dimensional contact characteristics (body's displacement $z(\tau)$, body's velocity $\dot{z}(\tau)$, contact pressure $p(\tau)$, contact temperature $\theta(\tau)$, and friction force $\varepsilon_1 F(\dot{z})p(\tau)$).

coefficient is decreased. Then, after some small delay, the contact pressure achieves its maximum, and the body begins to cool. When $\dot{z} = 0$, the slip phase is finished and the friction force achieves its maximal value, which makes a stick phase begin and the contact temperature, contact pressure and friction force decrease. The process stops when the frictional force achieves the value of the applied external force. Then the stick-slip process is repeated.

7. Conclusions

It this work the results concerning a novel problem of the so called "frog-slider" mechanical system that exhibits frictional thermo-elastic contact of a moving body subject to non-constant friction coefficients are presented and discussed. It is worth noticing that in the case of non-constant friction coefficient, self-excited vibrations can appear in the system without an elastic part (stiffness). This phenomenon is caused by the body heating during accelerating, the friction

increase, and then the braking and cooling of the system. The characteristic changes of both displacement (Fig. 6) and velocity of the analysed system are the reasons why the expression "frog-slider" coined to name the system seems appropriate.

Acknowledgements

This work has been partially supported by the grant of the State Committee for Scientific Research of Poland (KBN) No. TO7A01923.

References

[1] Mercalov NI. Dynamics of mechanisms. Moscow, 1913.
[2] Strelkov SP. Theory of the Froude pendulum self-vibrations. Journal of Technical Physics 1933;3(4):563–72.
[3] Wells JH. Kinetic boundary friction. Engineer (Great Britain) 1929;147:454.
[4] Thomas S. Vibration damped by solid friction. Philosophical Magazine 1930;9:329.
[5] Bowden FP, Leben L. The nature of sliding and analysis of friction. Proceedings of the Royal Society of London. Series A 1939;169:371–91.
[6] Van der Pol, B. Nonlinear theory of electric oscillations. 1934. Offprint from the Proceeedings of the Institute of Radio Engineers, vol. 22, Laboratoria N. V. Philips' Gloeilampenfabrieken. 8vo.: p. 1051–86.
[7] Kaidanovskiy NL, Khaikin SE. Mechanical relaxation vibration. Journal of Technical Physics 1933;3(1):91–107.
[8] Andronov AA, Vitt AA, Khaikin SE. Theory of oscillations. Oxford: Pergamon; 1966.
[9] Butenin NV, Neymark YI, Fufaev NA. Introduction to the theory of nonlinear vibrations. Moscow: Nauka; 1987.
[10] Blok H. Fundamental mechanical aspects of boundary lubrication. Society of the Automotive Engineering Journal 1940;46(2):54–68.
[11] Iszlinski AJ, Kragelsky IV. On jumps during friction. Journal of Technical Physics 1944;14:4–5.
[12] Kragelsky IV, Hittis N. Frictional self-oscillations. Moscow: Nauka; 1998.
[13] Antoniou SS, Cameron A, Gentle CR. The friction–speed relation from stick-slip data. Wear 1976;36:235–54.
[14] Martins JAC, Oden JT, Simões FMF. A study of static and kinetic friction. International Journal of Engineering Sciences 1990;28(1):29–92.
[15] Ibrahim RA. Friction-induced vibration, chatter, squeal and chaos. Part 1: mechanics of contact and friction. Part 2: dynamics and modeling. Applied Mechanical Review 1994;47(7):209–53.
[16] Pfeiffer F. Mechanische Systemen mit unstetigen Übergängen. Ingenieur-Achive Band 1984;54(3):232–40.
[17] Awrejcewicz J. Deterministic vibrations of lumped systems. Warszawa: WNT; 1996 (in Polish).
[18] Olędzki A, Siwicki I. Modelling of vibrations in a certain self-locking system. Proceedings XXXVI symposium modelling in mechanics, 1997. p. 265–8.
[19] Awrejcewicz J, Pyryev Yu. Influence of tribological processes on a chaotic motion of a bush in a cylinder-bush system. Meccanica 2003;38(6):749–61.
[20] Awrejcewicz J, Pyryev Yu. Thermoelastic contact of a rotating shaft with a rigid bush in conditions of bush wear and stick-slip movements. International Journal of Engineering Sciences 2002;40:1113–30.
[21] Olesiak Z, Pyryev Yu. Determination of temperature and wear during braking. Acta Mechanica 2000;143(1–2): 67–78.
[22] Ling FF. A quasi-iterative method for computing interface temperature distribution. Zeitschrift fur Angewandte Mathematik Physik 1959;10:461–74.
[23] Nowacki W. Thermoelasticity. Oxford: Pergamon Press; 1962.
[24] Carslaw HS, Jaeger JC. Conduction of heat in solids. Oxford: Clarendon Press; 1959.
[25] Abramowitz M, Stegun IA. Handbook of mathematical functions with formulas, graphs, and mathematical tables. New York: Dover; 1965.